

⁷Leger, T. J., Johnston, D. A., and Wolff, J. M., "Flex Circuit Sensor Array for Surface Unsteady Pressure Measurements," *Journal of Propulsion and Power*, Vol. 20, No. 4, 2004, pp. 754–758.

⁸Smith, S. N., "Discrete Frequency Sound Generation in Axial Flow Turbomachines," Aeronautical Research Council, R&M 3709, London, 1973.

Flex Circuit Sensor Array for Surface Unsteady Pressure Measurements

T. J. Leger,* D. A. Johnston,[†] and J. M. Wolff[‡]

Wright State University, Dayton, Ohio 45435-0001

Introduction

THE acquisition of high-fidelity, high-frequency response surface pressure measurements are of interest to experimentalists in gas-turbine aeromechanical research because these data provide a means to measure indirectly the unsteady aerodynamic loading acting on an airfoil. Airfoils are typically (traditionally) instrumented from commercially available miniature pressure transducers that are flush mounted to the airfoil to prevent the transducer from aerodynamically disturbing the flow. Cavities are machined into the airfoil to accommodate the transducers, and trenches are machined to route the lead wires away from the transducer.^{1–5} The main difficulty in the use of traditional transducers for high spatial resolution comes from the congestion and interference caused by the cavities and trenches required for each sensor location and the number of locations desired.

A high spatial resolution array of high-frequency pressure transducers was designed and fabricated that eliminates most of the difficulty associated with having a large concentration of transducers in a given area. Two pressure sensor arrays were applied to the suction and pressure surfaces of two inlet guide vanes (IGVs) of a transonic research compressor to measure the unsteady loading distribution induced by the passage of the bow shocks and the potential field emanating from the downstream rotor.

Flex Pressure Sensor Array

A high spatial resolution, high-frequency response flexible pressure sensor array was designed and fabricated. Two adjacent IGVs were instrumented with the flex pressure sensor array to capture the unsteady surface pressures associated with one vane passage. The sensors were arranged in a six spanwise \times five chordwise array. Figure 1 illustrates the locations of the sensors. Because the effects in the end wall boundary-layer regions are of interest, transducers extend to the 5 and 95% span locations.⁶ Earlier investigations indicated that the highest pressure fluctuations occur near the trailing edge of the IGV; hence, sensors were clustered near the trailing edge at the 95, 90, 85, 77, and 60% chord locations.¹

Flexible Circuit Substrate

The flex pressure sensor array design consists of two basic components, the flexible (flex) circuit substrate and the pressure sensor dies. The flex circuit substrate serves several purposes: first, it provides the electrical connections from the sensors (dies) to the outside

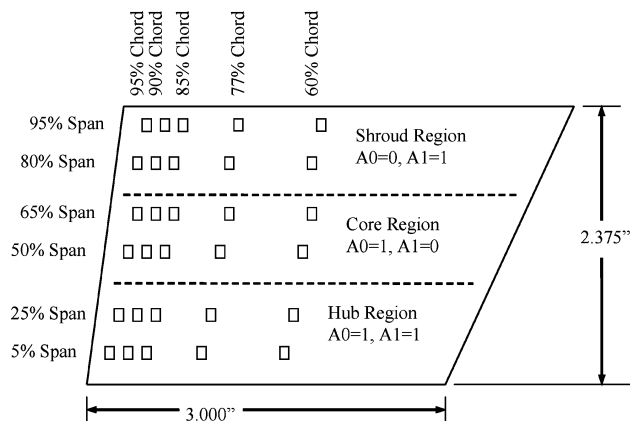


Fig. 1 Transducer locations.

of the rig in a slim, clean package, without the bundle of wires and machined trenches generally associated with instrumentation. Second, the flex circuit allows the sensor array to conform to the shape of the surface to which it is adhered. In this case, a simple shallow face 0.030 in. (0.762 mm) deep was machined into the IGV surface to compensate for the thickness of the flex substrate to allow flush mounting with the vane surface.

The flexible circuit substrate also enables the sensors to be packed to give a high spatial resolution because the wire locations for each sensor are precisely controlled. That is, individual trenches are not machined into the blade surface. Also, it provides several other significant cost benefits: First, the cost of instrumenting the blade on a per-sensor basis is decreased. The flex sensor array, including the machining and mounting, costs \$42,000 or \$700/sensor. The previous instrumentation by Probasco et al. cost \$1250/sensor.¹ Second, the cost associated with the added complexity of connecting four individual wires for each sensor to the data acquisition system is significant when compared to utilization of the flexible circuit substrate, which only requires two connections. Although an exact dollar value cannot be calculated, the savings in terms of time and potential errors and failure modes are significant.

Two mirror-image circuit layouts were required for the suction and pressure surfaces of the adjacent vanes. A three-layer design was used: The bottom layer contains all of the traces, that is, thin film conductors, for sensor signal output. A middle layer contains all of the traces for sensor power input. The top layer contains the pads on which the sensor dies are mounted and connections to the data acquisition system are attached. To reduce the number of traces required, the negative excitation (ground) for all sensors in the array row were ganged together. Electrical connection of the flex circuit to the data acquisition system is provided by edge-board connectors with 0.050-in. (1.27 mm) spaced fingers, thereby precluding the need to solder 240 individual wires and allowing the flex circuit neck to be easily inserted through a slot in the outer casing of the rig during installation.

After the flex circuit layout was designed, it was sent to Dynamic FPC for conversion to Gerber format, a format used by printed circuit board manufacturers to apply the circuit trace masks via special plotting. The Gerber data were then sent to the Tyco Printed Circuit Group for manufacture of the flex circuit. Each layer of the design is made by first adhering a thin, 1-oz. copper film to a 0.001-in. (0.0254 mm) Kapton[®] sheet. The copper film is then masked and etched by the use of standard industry printed circuit board techniques. The typical size of the flex circuit traces is 0.007-in. (0.1778 mm) width with a spacing of 0.006 in. (0.1524 mm) between the traces in some areas. Small donut-shaped conductors called vias are used to connect one layer to the next. After etching, the three layers are aligned with the aid of small alignment holes and adhered together. Following this, the vias between different layers are connected by small amounts of conductive epoxy. Finally, the exposed copper pads are electroplated with 30 μ -in. (762 nm) of gold, ensuring good conductivity with the sensor dies and the

Received 30 September 2002; revision received 5 April 2004; accepted for publication 5 March 2004. Copyright © 2004 by the authors. Published by the American Institute of Aeronautics and Astronautics, Inc., with permission. Copies of this paper may be made for personal or internal use, on condition that the copier pay the \$10.00 per-copy fee to the Copyright Clearance Center, Inc., 222 Rosewood Drive, Danvers, MA 01923; include the code 0748-4658/04 \$10.00 in correspondence with the CCC.

*Graduate Research Assistant, Department of Mechanical and Materials Engineering. Student Member AIAA.

[†]Research Associate Professor, Department of Mechanical and Materials Engineering. Member AIAA.

[‡]Professor, Department of Mechanical and Materials Engineering. Associate Fellow AIAA.

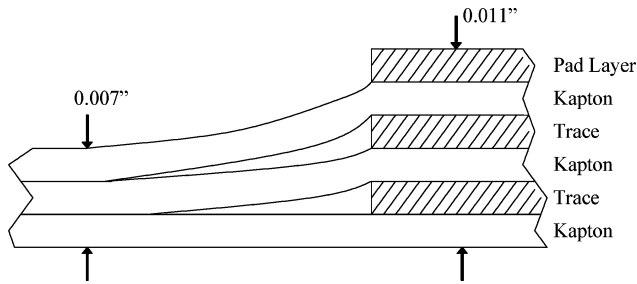


Fig. 2a Transducer die dimensions.

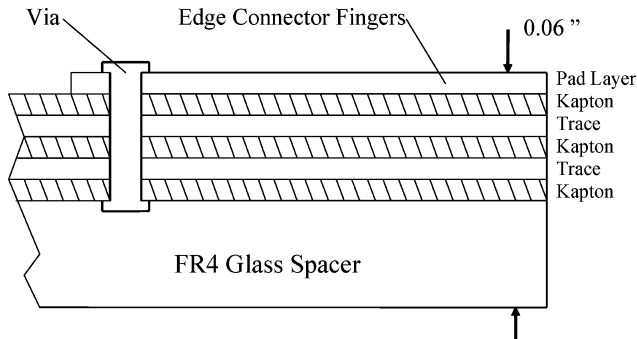


Fig. 2b Flex circuit layering near sensors.

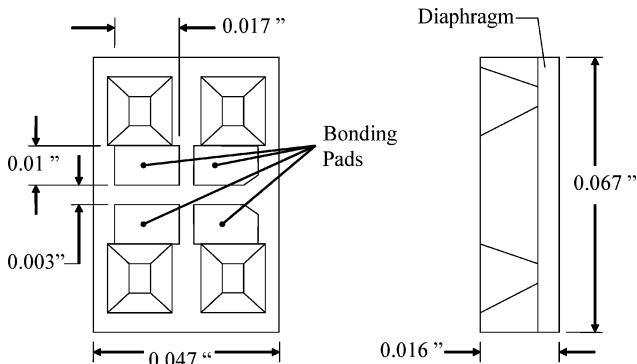


Fig. 2c Flex circuit layering near edge connectors.

edge-board connectors. The total thickness of the flex circuit, as shown in Fig. 2a, is 0.011 in. (0.2794 mm) at the sensor region, with a thickness of 0.007 in. (0.1778 mm) away from the sensor, and a thickness of 0.060 in. (1.524 mm) for the edge-board connector (Fig. 2b).

The two flex circuits were then adhered with 3M brand adhesive film to the shallow faces machined into the vanes. The vanes were sent to Endevco for mounting of the sensor dies and final fabrication. A photograph of the flex circuit after manufacture is shown in Fig. 3.

Pressure Sensor Dies

Endevco was chosen as the vendor for the manufacture and mounting of the high-frequency response pressure sensor dies because Endevco had experience from its manufacture of a similar device, the “pressure belt” strip.^{7,8}

The dimensions of the pressure sensor die are $0.047 \times 0.067 \times 0.016$ in. ($1.194 \times 1.702 \times 0.406$ mm) as shown in Fig. 2c, with technical specifications presented in Table 1. The dies feature a sealed cavity on the backside of the diaphragm, allowing the sensors to measure absolute pressures via a reference vacuum sealed in this cavity during manufacture.

A unique feature of this die is the method by which it is mounted, the so-called flip-chip technique. Conventional sensor dies use thin aluminum wires for the connection from the die to the electrical

Table 1 8515c-15 sensor specifications

Sensitivity	13.3 (8.67) mV/psi typical (min)
Burst pressure	75 psia min
Excitation	10.0 Vdc
Full-scale output	200 (130) mV (min)
Impedance: input	2700 Ω typical, 2000 Ω min
output	1500 Ω typical, 2200 Ω max
Resonance frequency	180 kHz
Nonlinearity at three times range	1.0% three times full scale output (FSO) max
Zero shift after three times range	$\pm 0.5\%$ three times FSO max
Acceleration sensitivity	0.0002 psi/g
Nonrepeatability	0.1% FSO typical
Pressure hysteresis	0.1% FSO typical
Nonlinearity	0.2% FSO typical
Thermal sensitivity shift	$\pm 3\%$ FSO max
Thermal zero shift	$\pm 2.5\%$ FSO max

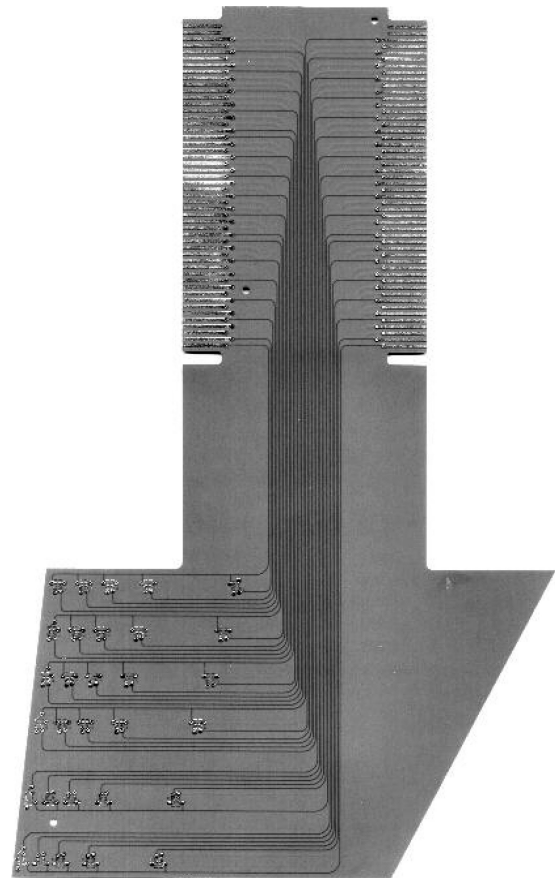


Fig. 3 Manufactured flex circuit.

substrate. These wires tend to fatigue and break over time due to stress and strain from the small movement of the dies relative to the substrate. Also, these aluminum wires typically attach to the top of the sensor die and extend past the surface of the diaphragm, making the packaging thicker. To eliminate these potential problems, the flip-chip technique utilizes pads on the bottom of the die, which are attached to the electrical substrate via conductive epoxy. Each pad measures 0.010×0.008 in. (0.254×0.203 mm).

In packaged form the Endevco sensor dies are designated as the 8515c family of sensors. The die comes in two pressure ranges, 15 and 50 psia (344.7 kPa). Based on previous IGV experimental data by Probasco et al. the 15-psia (103.4 kPa) range sensor was specified for the instrumented vanes.¹

Because these sensors are to make nonintrusive surface pressure measurements, the surface of the sensor array was specified to be as smooth as practicable. A lamination of a thin, rubber sheet and Kapton tape with cut outs at the sensor locations facilitated this goal

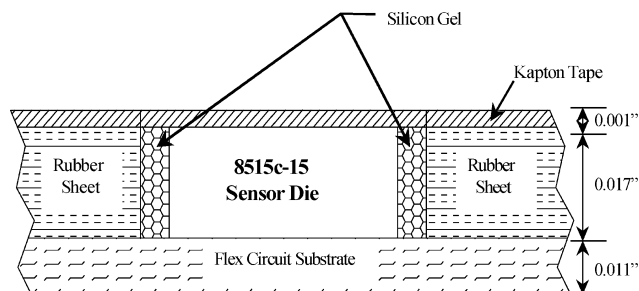


Fig. 4 Cut-away view at a sensor location.

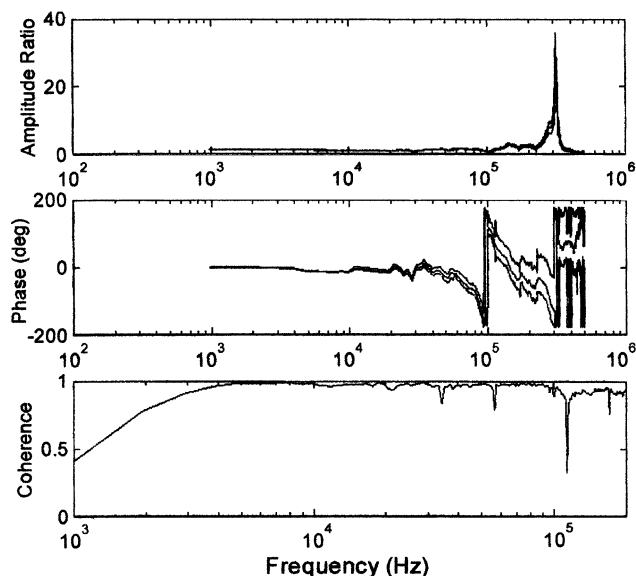


Fig. 5 Dynamic calibration plot.

by filling in the bulk of the recessed area left over once the sensor dies were attached. Silicon gel was then applied between the rubber sheet and the sensor dies to produce a smooth surface with no significant voids or bumps visible. Figure 4 shows the final assembly.

Dynamic Sensor Response

Dynamic response of the 8515c-15 sensor was determined by tests of two sample sensors in the Wright State University (WSU) Shock Tube. Whereas the samples tested in the shock tube used the traditional aluminum wire technique for connection of the sensor to the substrate, the sensors were mounted without screens to one of the shock tube aluminum test plates with 3M adhesive tape. In the shock tube tests, the sensors were exposed to a 5-psi pressure step, and their responses were captured by a high-speed data acquisition system sampling at 1 MHz. More details of the WSU shock tube system and data analysis methods are given by Kobayashi.⁹ The captured time traces were then Fourier analyzed, as shown in Fig. 5. Results indicate a usable frequency bandwidth of 30 kHz. The maximum blade passing frequency of interest is 7.4 kHz; thus, the sensors should capture, with fidelity, unsteadiness within the first four harmonics of blade passing frequency.

Multiplexer Array

The pressure sensor array contains 60 transducers that must be measured with 20 available channels of the data acquisition system. A multiplexing circuit was, therefore, designed to interrogate the sensor array. The sensors were divided into three groups of 20 (Fig. 1) and multiplexed to the data acquisition system via a bank of four-channel, differential, DG409 multiplexers (MUX). In addition, the MUX boards incorporate a set of 1360- Ω low thermal coefficient of resistance (TCR) resistors to minimize the thermal drift of the pressure sensors. A schematic showing the layout for each MUX in the array is given in Fig. 6.

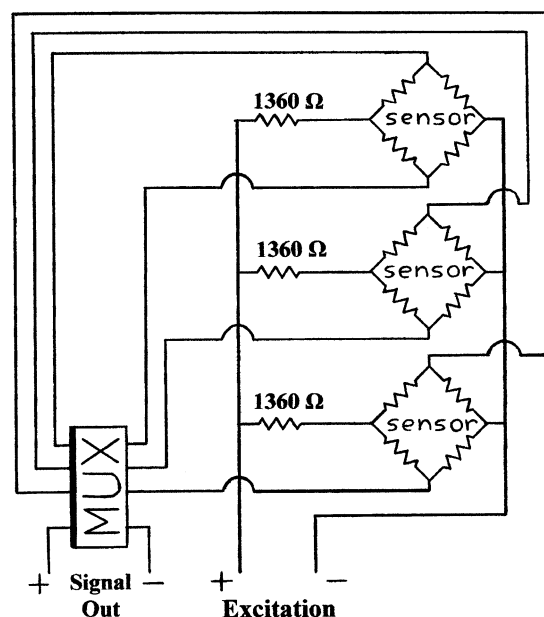


Fig. 6 Connection schematic for each MUX.

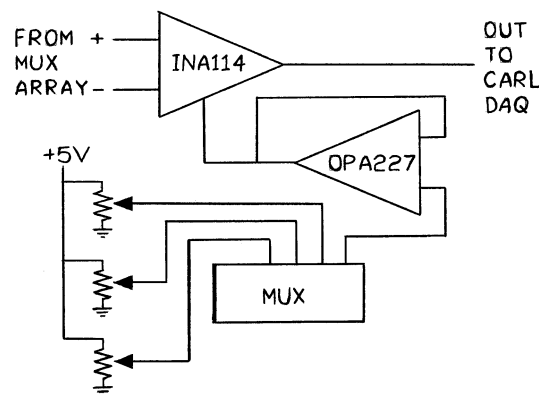


Fig. 7 Trimmer circuit schematic for one sensor set.

Trimmer Circuits

During preliminary static calibration of the instrumented vanes using the MUX circuitry, the data acquisition signal conditioners became saturated in the upper-half of the calibration pressure range when moderate gains were used. The cause of the saturation was traced back to dc offset of the sensors, which exceeded the limits of the signal conditioners. To correct the problem, a pair of trimmer circuits was designed and constructed. The trimmer circuit is incorporated between the 40-pin integrated device connector (IDC) headers of the MUX boards and the data acquisition system. The trimmer circuits allow the dc offset of each sensor to be adjusted to within a few millivolts of zero, allowing much higher gains to be applied to the unsteady pressure signal before recording to tape.

A schematic diagram for one set of sensors is shown in Fig. 7. The circuit consists of an INA114 instrumentation buffer amplifier. A set of potentiometers is used to trim the offset voltage, which is then passed through an OPA227 general-purpose amplifier that serves as a voltage follower. To select which potentiometer value is used with each sensor, a MUX was incorporated into the design. The instrumentation amplifier and voltage-follower combination provide isolation from the rest of the circuit, along with very high input impedance for the sensors.

Calibration

Static calibration was performed on the system comprised of the instrumented vanes, MUX array, trimmer circuits, and data acquisition electronics. The instrumented vanes were sealed in a pressure chamber with the pressure level controlled by a DRUCK DPI 510

electronic pressure regulator connected to both vacuum and pressurized air sources. An effective gain of 400 was used with the sensor dc output voltage zeroed at 11 psia (75.8 kPa), the anticipated mean pressure at the vane during compressor operation. Calibrations were performed from 6 to 16 psia (41 to 110 kPa) in 1-psi (6.89 kPa) increments, resulting in an ~ 1 V/psi sensitivity. To account for thermal shift and repeatability, the calibrations were performed several times at 55 and 75°F (12.8 and 23.9°C) (the target compressor operation temperature range) as measured by a thermocouple installed in the pressure chamber. By the use of the sensor specification in Table 1, the maximum error would be ± 0.6 psi (4.1 kPa), mostly due to thermal sensitivity and zero shift. However, the calibration showed an error of only ± 0.07 psi (0.5 kPa), which clearly indicates the importance of the low TCR resistors added to the MUX array. In addition, analysis of floor data (zero-excitation signal taken before the experiment) showed a maximum error of ± 0.1 psi (0.7 kPa),

which includes all electrical noise and temperature changes for the experimental setup. A calibration curve of one sensor set is shown in Fig. 8, illustrating the linearity of the sensors.

Installation and Data Acquisition

After calibration, the instrumented vanes were installed in the compressor rig, as shown in Fig. 9. During testing, the signals from the pressure sensor array were recorded to a 28-track Datatape model 3700J analog tape deck operating at 120 in./s (3.048 m/s). When the signals were digitized after testing, the tape was played back at 40 in./s (1.016 m/s), effectively quadrupling the digitization rate. Following the digitization of the signals, the digitized data were ensemble averaged on the time basis of the rotor revolution period, by the use of the time traces of 219 rotor revolutions. Ensemble averaging eliminates the high-frequency fluctuations due to incoherent unsteadiness associated with turbulence and, thereby, clarifies the stationary periodic unsteadiness that is of interest.

Durability

During calibration and testing of the flexible pressure sensor array, a total of 10 of the original 60 sensors failed. A number of these failures can be attributed to an accident in which one of the flex circuits ripped due to excessive handling during the calibration. As a result, seven sensors lost electrical connectivity to the edge connector fingers. An attempt to repair the flex circuit with 0.003-in. (0.0762 mm)-diam wire resulted in five of the sensors being recovered. However, during testing, electrical contact to three of the five repaired circuits was lost. In addition to these losses, two sensors were damaged during the calibration. Finally, three additional sensors were lost during the three-day testing in the compressor rig.

Summary

In this Note, the design of a high spatial resolution, flex pressure sensor array was presented, constructed to measure the unsteady surface pressures acting on the IGVs of a transonic compressor rig. The sensor arrays were constructed of two thin, flexible, circuit substrates adhered to two IGVs and mounted with 30 high-frequency response pressure transducers each. Also included were the details of the design and construction of the electronic circuitry for interrogating the 60 transducers during data acquisition. Finally, a significant cost saving of 44% in instrumentation of the IGV was realized over

DAQ Channel 1

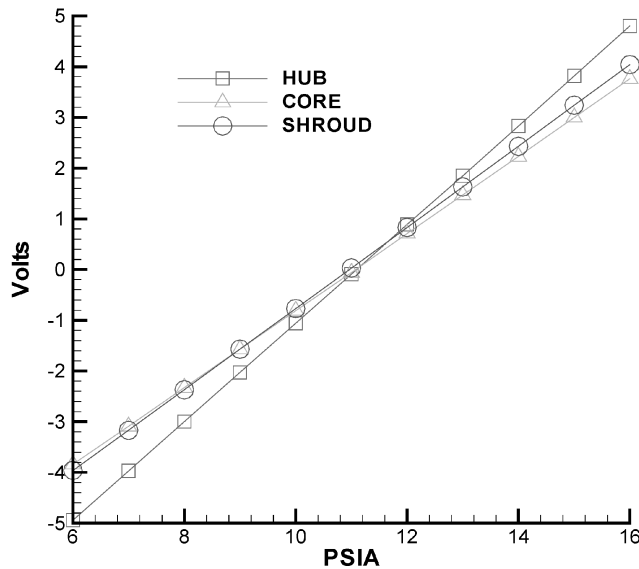


Fig. 8 Typical static calibration plot.

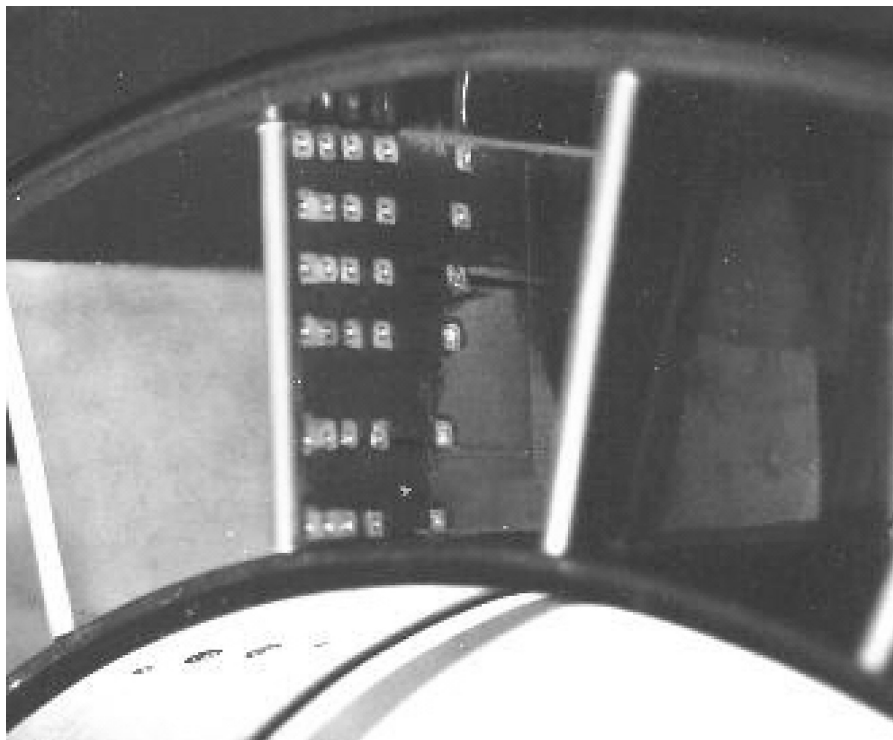


Fig. 9 Installed instrumented vane.

traditional instrumentation methods, along with substantial benefits in the handling of the sensor wiring.

Acknowledgments

U.S. Air Force (USAF) Contract F33615-98-C-2895, with Technical Monitor Charles Cross, and the Dayton Area Graduate Studies Institute Project PR-AFIT-99-07 sponsored this research. Their support is most gratefully acknowledged. In addition, the support of the Compressor Aero Research Laboratory staff and use of the U.S. Air Force facility is acknowledged.

References

- ¹Probasco, D. P., Leger, T. J., Wolff, J. M., Copenhaver, W. W., and Chriss, R., "Variations in Upstream Vane Loading with Changes in Back Pressure in a Transonic Compressor," 2000, *Journal of Turbomachinery*, Vol. 122, No. 3, pp. 433–441.
- ²Sanders, A., and Fleeter, S., "Forcing Function Variability and Its Effect on Airfoil Response," AIAA Paper 98-3898, July 1998.
- ³Manwaring, S. R., and Wisler, D. C., "Unsteady Aerodynamics and Gust Response in Compressors and Turbines," *Journal of Turbomachinery*, Vol. 115, No. 4, pp. 724–740.
- ⁴Rao, K. V., Delaney, R. A., and Dunn, M. G., "Vane-Blade Interaction in a Transonic Turbine, Part I: Aerodynamics," *Journal of Propulsion and Power*, Vol. 10, No. 3, 1994, pp. 305–311.
- ⁵Dring, R. P., Joslyn, H. D., Hardin, L. W., and Wagner, J. H., "Turbine Rotor-Stator Interaction," *Journal of Engineering for Power*, Vol. 104, Oct. 1982, pp. 729–742.
- ⁶Koch, P. J., Moran, J., and Wolff, J. M., "3-D Inlet Guide Vane Generated Vortical Forcing Functions," *International Journal of Turbo and Jet Engines*, Vol. 17, No. 4, 2000, pp. 289–302.
- ⁷Karolys, A., and Swanson, B., "The Pressure Belt: A Smart Sensor Network System," *NASA Tech. Briefs*, Vol. 23, No. 10, Oct. 1999, pp. 72, 73.
- ⁸Swanson, B., "Smart Pressure Belt," *Design News*, Vol. 54, No. 17, Sept. 1999, pp. 71, 72.
- ⁹Kobayashi, H., "Unsteady Pressure Measurement Issues for High Speed Turbomachinery Applications," M.S. Thesis, Dept. of Mechanical Engineering, Wright State Univ., Dayton OH, Sept. 1999.

Studies on Ferrocene Polyglycol Oligomer—Burning-Rate Modifier for Composite Propellants

G. M. Gore,* R. G. Bhatewara,† K. R. Tipare,‡
A. N. Nazare,§ and S. N. Asthana¶
High Energy Materials Research Laboratory,
Pune 411021, India

Introduction

L IQUID-FERROCENE derivatives have evinced great interest as burning-rate catalyst for ammonium-perchlorate (AP)-containing composite propellants. A major advantage of these speciality materials over conventionally used solid catalysts (Fe_2O_3 or copper chromite) is that they do not impose penalty on loading of the energy-producing solid oxidants and fuels.¹ However, a widely used ferrocene derivative, namely, n-butyl ferrocene (nBF),

tends to migrate during storage, resulting in changes in programmed burning rates leading to reduction in useful life of the propellant. Moreover, air oxidation of nBF migrated to the surface converts it to products rendering propellants susceptible to impact and friction stimuli. One of the approaches to mitigate migration problem is to select ferrocene derivatives carrying large and bulky substituents. This led to the emergence of 2,2' bis(ethyl ferrocenyl propane) [catocene] and 1,3 di ferrocenyl-1-butene (DFB)^{1,2} as an alternate choice. However, the problem of migration exists for them through to a lesser extent. A major technological breakthrough was achieved at SNPE, France, with the development of technology of BUTACENE obtained by grafting ferrocene moiety on pendant $-\text{CH}=\text{CH}_2$ of hydroxyl-terminated-polybutadiene (HTPB) prepolymer.³ Another innovative approach involves modification of ferrocene molecule by introducing reactive isocyanate or hydroxyl groups,⁴ which can get bonded to the end groups of the polymeric binders through curative during the course of curing of polymer/propellant. Nilesen⁵ has reported use of functional di ferrocenyl compounds.

Manke et al.⁶ demonstrated that ferrocene compounds containing a single hydroxyl end group are as effective (or even more) as catocene in enhancing the burning rates of composite propellants.

This Note reports synthesis and characterization of ferrocene polyglycol oligomer (FPGO) having reactive hydroxyl ($-\text{OH}$) end groups capable of chemically bonding to HTPB by the agency of isocyanate curatives through urethane bridge. Potential of FPGO vis-à-vis nBF and DFB was evaluated as burning-rate enhancer for AP-HTPB composite propellants during this work. Fe_2O_3 was also evaluated to generate the reference data. Thermal studies were undertaken to get information on decomposition pattern of ferrocenes and the propellants.

Experimental

Synthesis and Characterization of FPGO

FPGO was synthesized on the lines of the method reported in patent.⁷ The synthesis involved condensation of ferrocene with acetyl chloride in the presence of AlCl_3 leading to the formation of diacetyl ferrocene (DAF). DAF was converted to bis (hydroxy ethyl) ferrocene (BHEF) on reduction by sodium borohydride (NaBH_4) in isopropanol. Condensation of BHEF with 1,4 butane diol in the presence of BF_3 etherate yielded FPGO. Synthesized material was characterized by ultra violet-near infrared (UV-NIR) (Hitachi model 340-C) in acetonitrile, Fourier transformed infrared (FTIR) (Perkin Elmer Model 1605) in KBr pellet, and ^1H Nuclear Magnetic Resonance (^1H -NMR) (Bruker 300 MHz) in CDCl_3 . Iron content was determined by colorimetric estimation. Number average molecular weight (M_n) was obtained on a vapour-pressure osmometer (KANUER make), and viscosity was measured on Brookfield viscometer (model DV-3). DFB was synthesized and characterized as per the methods reported earlier,⁸ whereas nBF and Fe_2O_3 (mean average particle size 5μ) were obtained from commercial source and used as such to generate comparative data.

Processing of Propellant

Composite propellant selected for the present study comprised 85% AP and 15% binder {prepolymer-HTPB 7.5%, plasticizer-diethyl adipate-DOA 4.5%, antioxidant cum cross linker-pyrogallol 0.5%, process aid-lecithin 0.3% and curative-toluene di isocyanate-TDI 2.2% [isocyanate (NCO):Hydroxyl (OH) 1:1]}. HTPB, DOA, and pyrogallol were mixed under vacuum (10 torr) for 2 (h). Bi-modal (60:40 blend of 250μ and 9μ size) or monomodal fine (9μ) AP was added to the binder, and mixing was continued for 30 min. Burning-rate catalysts (Fe_2O_3 /nBF/DFB/FPGO) were incorporated into one to two parts by weight over 100 parts of the composition and mixed for 10 min. Subsequently, curative (TDI) was added, and final mixing of the contents was carried out for 45 min (including 15 min under vacuum). The slurry was cast in a mould evacuated to <10 torr and cured at $60 \pm 2^\circ\text{C}$ for 10 days. All of the solid ingredients were dried to the moisture level of $<0.5\%$ before processing. Particle size of AP was determined on Malvern particle size analyser (Model Series 2600 C). The 80% particles fall at mean average value.

Received 3 December 2002; revision received 29 October 2003; accepted for publication 5 December 2003. Copyright © 2004 by the American Institute of Aeronautics and Astronautics, Inc. All rights reserved. Copies of this paper may be made for personal or internal use, on condition that the copier pay the \$10.00 per-copy fee to the Copyright Clearance Center, Inc., 222 Rosewood Drive, Danvers, MA 01923; include the code 0748-4658/04 \$10.00 in correspondence with the CCC.

*Scientist 'D.'

†Technical Officer 'A.'

‡Technical Officer 'A.'

§Technical Officer 'C.'

¶Scientist 'F,' Group Director.